ELSEVIER

Polymer 41 (2000) 8311–8320

polymer

www.elsevier.nl/locate/polymer

Phase separation and gelation behaviors in poly(vinylidene fluoride)/tetra(ethylene glycol) dimethyl ether solutions

Po-Da Hong*, Che-Min Chou

Department of Textile and Polymer Engineering, National Taiwan University of Science and Technology, Taipei 10607, Taiwan, ROC

Received 29 November 1999; received in revised form 31 January 2000; accepted 13 March 2000

Abstract

In this work, the phase separation and gelation behaviors in poly(vinylidene fluoride)/tetra(ethylene glycol) dimethyl ether (PVDF/TG) solutions were studied through the time-resolved light scattering and the gelation kinetic analyses. Combination of the phase diagram and the results of gelation kinetics shows that the gelation behaviors in PVDF/TG solutions could be separated into three diverse regions. According to the initial thermodynamic conditions, one can divide the gelation processes into two major parallel reactions. At the gelation temperature above the spinodal temperature ($T > T_s$), the gelation should be virtually independent of phase separation and then the gelation should occur in terms of bimolecular association and pure crystalline nucleation. When $T < T_s$, the crystallization and phase separation occur simultaneously and the gelation depends on the kinetic conditions of two competitive processes. Two gel regions could be separated by a kinetic transition concentration, C^*_{trans} which is obtained from various rate-determining mechanisms at the gelation temperature below T_s. When the lower concentration PVDF solutions undergo spinodal decomposition, the phase separation is the rate-determining step on the gelation and is known as diffusion control. Meanwhile, the nucleation or reaction control is the rate-determining step for the higher concentration ones, indicating that the influence of phase separation on the gelation behavior may be weakened when the concentration is increased beyond C^*_{trans}.

Keywords: Poly(vinylidene fluoride); Phase separation; Spinodal decomposition

1. Introduction

Thermoreversible physical gel is a three-dimensional network of polymer chains cross-linked by physical association. It is well known that many factors affect the gelation behavior of polymer solution, such as the temperature, the concentration of polymer, and the type of solvent used [1–3]. Therefore, it is of considerable interest to undertake the kinetic study of how the structure forms during gelation. Generally, three fundamental mechanisms could be considered for the gelation behavior, i.e. the liquid–liquid phase separation by spinodal decomposition [4,5], the liquid–solid phase transition by crystallite formation of the polymer chain segments [6,7] and the percolation type association [8]. Actually, the mechanisms of structural formation for polymer physical gels are so complex that the extremely subtle gelation phenomena have still have not been fully elucidated. Ransil et al. [4] have studied the kinetics of spinodal decomposition in gelatin/water/methanol mixture, which undergoes a gelation simultaneously with phase separation. Their results suggest that when gelation and phase separation occur simultaneously the kinetics and morphology depend on the location of temperature and on the rates of phase separation and gelation. Similar results have also been found for PVDF/PMMA blends [9]. This study applied the concept of the kinetic analysis of two competitive processes to interpret the crystallization affected by the liquid–liquid phase separation. However, there are no quantitative analyses for the influences of thermodynamic and kinetic conditions on the initial gelation behaviors.

In this work, the relation between the phase separation behavior and gelation kinetics in PVDF/TG solutions was first studied. The mechanism and characterization of gelation and the dependence on temperature and concentration are also discussed in this work.

2. Experimental

2.1. Materials

Poly(vinylidene fluoride) (PVDF) powder ($M_w = 543,000$,

* Corresponding author. Tel.: + 886-2-273-76539; fax: + 886-2-273-76544.

E-mail address: phong@hp730.tx.ntust.edu.tw (P.-D. Hong).

0032-3861/00/$ - see front matter
PII: S0032-3861(00)00196-8

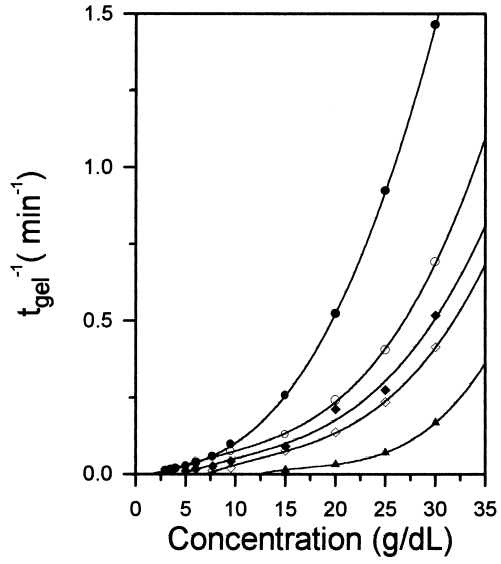

Fig. 1. Apparent gelation rate, t_{gel}^{-1} as a function of concentrations for PVDF/TG solutions at various temperatures: (●) 30°C; (○) 40°C; (◆) 60°C; (◇) 70°C; (▲) 80°C.

Aldrich Chem. Co., USA) was used in this work. The solvent, tetra(ethylene glycol) dimethyl ether (TG) was first dried by using 3 Å molecular sieve and then filtered by using 0.02 μm Teflon filter for removing dust. The homogeneous PVDF solutions were prepared by dissolving the PVDF powder at 180°C in sealed test tubes which were then quenched to the ambient temperature for measurements.

2.2. Measurements

2.2.1. Gelation rate

Firstly, PVDF solutions with various concentrations in sealed test tubes were kept in an oven at 180°C for about 1 h to make the solutions homogeneous before measuring. Then the hot solutions were quickly transferred into a water bath kept at a given temperature, controlled within ±0.1°C. The test tube tilting method was used for determining the gelation time (t_{gel}), which was defined by observing the cessation of the solution flow inside the test tube when it was tilted. The reciprocal of gelation time of the solution is referred as the apparent gelation rate, t_{gel}^{-1}.

2.2.2. Gel melting temperature

The test tube upside-down method was used to determine the gel melting temperature (T_m^g) of PVDF gels prepared from various concentrations. The solutions were prepared in sealed test tubes and heated until they turned homogeneous. The solutions were quenched to 30°C for one day to form gels. The test tube with the gel was kept upside down in a thermostat oven at a heating rate of 1°C min^{-1} so as to allow even heating. The temperature at which the gel begins to flow was defined as the T_m^g of the gel.

2.2.3. Time-resolved light scattering

The measurement was carried out using a Malvern series 4700 apparatus; the light source was a 25 mW He–Ne laser with a wavelength of 633 nm with vertically polarized light, which was focused on the sample cell through a temperature-controlled chamber (the temperature being controlled to within ±0.1°C) filled with distilled water. The hot homogeneous solutions were quickly quenched in a water-bath at constant temperature and then kept for 1 min to stabilize the solutions before light-scattering measurements. The time dependence of scattered intensity during the isothermal phase was measured using the step-scattering measurement in the scattering vector (q) range of 2.012×10^{-5} $cm^{-1} \leq q \leq 2.674 \times 10^{-5}$ cm^{-1} [$q = (4\pi n/\lambda) \sin(\theta/2)$, where θ is the scattering angle, n is the refractive index of the medium and λ is the wavelength of incident light].

3. Results

3.1. Kinetics of gelation

The apparent gelation rate is obtained from the reciprocal of gelation time, t_{gel}, which is the time required for the polymer solutions to form the gels. Fig. 1 shows the t_{gel}^{-1} values of the PVDF/TG solutions as a function of polymer concentration at various gelation temperatures. The result shows that the t_{gel}^{-1} increases with increasing concentration and with decreasing temperature. In order to determine the critical concentration for gelation, C_{gel}^*, which is an important parameter to understand the mechanism of gelation, all curves in Fig. 1 were extrapolated to zero gelation rate. The C_{gel}^* value apparently depends on the gelation temperature. Generally, the gelation of polymer solutions should tack place above the chain overlapping concentration, C^*. Oukura et al. [10] have studied the gelation of PVA in a DMSO/water mixture and pointed out that the chain overlap concept can be applied to gelation from a homogeneous polymer solution and the C^* or C_{gel}^* was considered to be independent of temperature. However, the C^* value is disagreeing with the C_{gel}^* value and depends on the temperature for PVA gels formed at certain temperature region implying that the liquid–liquid phase separation or spinodal decomposition may strongly affect the gelation behavior. According to the observations in PVA solutions as mentioned above, the gelation process of the PVDF/TG solution may also be concerned with the liquid–liquid phase separation. In this work, the gelation rate of PVDF/TG solution depends on the concentration and also on the gelation temperature. Hence, t_{gel}^{-1} can be expressed as a combination of the concentration and temperature function [11,12]

$$t_{gel}^{-1} \propto f(C)f(T) \tag{1}$$

In order to give a general character of the concentration function, the reduced concentration and the exponent n

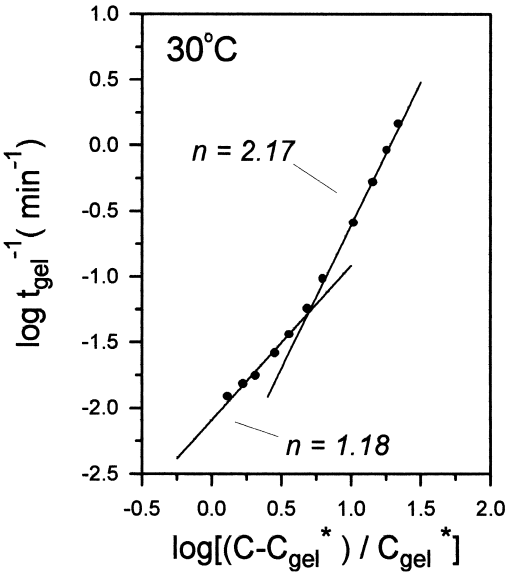

Fig. 2. log t_{gel}^{-1} versus log[$(C - C_{gel}^*)/C_{gel}^*$] plot of PVDF/TG gel at 30°C.

should be introduced. Therefore, at a given temperature the gelation rate can be given as a general relationship by writing

$$t_{gel}^{-1} \propto [(C - C_{gel}^*)/C_{gel}^*]^n \quad (2)$$

where n is an exponent value depending on the gelation mechanism.

Fig. 2 shows the double logarithmic plots of t_{gel}^{-1} as a function of reduced concentration at 30°C. Two different rate-dependent regions were found at low and high concentrations and the n values, obtained from the slope of each concentration region, are about 1 and 2, respectively. This discrepancy may be ascribed to the fact that the gelation behavior in PVDF/TG solution possesses various kinetic processes. Ohkura et al. [12] studied the gelation rate on PVA solution and reported that the exponents value "2" could be regarded as the binary association of segments in the cross-linking loci. However, it is presently difficult to explain the physical meaning of the exponent value "1" for the gelation process in PVDF/TG solutions. The kinetic transition concentration, C_{trans}^*, could be determined from the intersection of two straight lines. These characteristic values of C_{gel}^*, C_{trans}^* and n for the kinetic processes of gelation are summarized in Table 1.

Table 1
The critical gelation concentration C_{gel}^*, transition concentration $C_{trans}^*$and exponent n values for PVDF/TG gels

T_{gel} (°C)	C_{gel}^* (g dl^{-1})[a]	C_{trans}^* (g dl^{-1})[b]	n_1	n_2
30	1.3	7.7	1.18	2.17
40	1.6	9.5	0.95	2.15
60	4.5	12.5	0.98	1.97
70	7.0	15.8	0.93	1.93
80	12.2			2.00
85	13.0			1.98
90	14.5			1.95
Average			1.01	2.02

[a] Obtained in this work by extrapolation to $t_{gel}^{-1} = 0$.
[b] The transition concentration was determined from the intersection of two lines from the plots of log t_{gel}^{-1} versus log[$(C - C_{gel})/C_{gel}$] in Fig. 2.

3.2. Spinodal decomposition

As mentioned above, since the C_{gel}^* value evidently depends on the gelation temperature, it is likely that the gelation of PVDF/TG solutions occurs in the heterogeneous solution caused by phase separation. The spinodal decomposition mechanism at the initial stage of phase separation could be described well through Cahn's linear theory [13,14]. The scattered intensity is then given as follows:

$$I(q,t) = I(q,t=0)\exp[2R(q)t] \quad (3)$$

where $I(q,t)$ is the scattered intensity at a given scattered vector q and time t. The $R(q)$ value which is the growth rate of concentration fluctuation, is given by

$$R(q) = D_c q^2\left\{-\frac{\partial^2 f}{\partial C^2} - 2\kappa q^2\right\} \quad (4)$$

where D_c is the cooperative diffusion coefficient of polymer chains in solution, f is the free energy of mixing, C is the concentration of solution, and κ is the concentration-gradient energy coefficient defined by Cahn. According to Eq. (3), the exponential increase in the scattered intensity with time can be described by a linear theory. Fig. 3 shows the change in the logarithm of the scattered intensity as a function of time at various scattering vectors for 3.2 g dl^{-1} PVDF/TG solution at 30°C. From Fig. 3 the ln(I) versus t sigmoid curve could be separated into three various regions. Firstly, the induced period of the liquid–liquid phase separation was found in which the scattered intensity shows no remarkable change with time. Then, the scattered intensity increases exponentially with time. Finally, the scattered intensity deviates from the exponential relationship. This deviation is considered to be a consequence of the coarsening effect at the later stage of spinodal decomposition, which has been discussed in many studies [15,16]. The result in Fig. 3 shows that the ln(I) versus t relationship is indeed linear after the induced time. Therefore, we assume that this result might be suitable to be described by Cahn's linear theory. According to the linear theory described by Eq. (3), one can estimate the concentration fluctuation rate $R(q)$ at a given q value from the slope of straight line in the plot of ln(I) versus t, the slope yielding $2R(q)$, as shown in Fig. 3. Linear results were also obtained for other solutions with various concentrations and temperatures.

Fig. 4 shows the result of $R(q)/q^2$ as a function of q^2 based upon Cahn's linear theory for 3.2 gd l^{-1} PVDF/TG solution at various temperatures. Fairly good linear relationships were obtained. From the plots and Eq. (4) one can estimate the characteristic parameters which describe the dynamics of the phase separation such as, the apparent diffusion

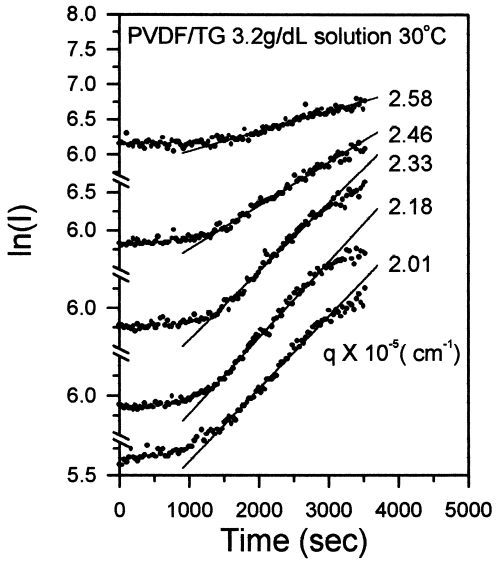

Fig. 3. Time evolution of the logarithm of the scattered intensity at various q measured for 3.2 g dl^{-1} PVDF/TG solution at 30°C.

coefficient, $D_{app} = -D_c(\partial^2 f/\partial C^2)$, from the intercept of $R(q)/q^2$ at $q = 0$; q_c, the most probable wavenumber of fluctuations that can grow, from the intercept of q^2 at which $R(q)/q^2 = 0$, and q_m, the most probable wavenumber of fluctuations that can grow at the highest rate, q_m being estimated from $q_m = q_c/2^{1/2}$. These calculated parameters are summarized and shown in Table 2. In order to check such a spinodal decomposition, the $R(q)$ value was plotted as a function of q as shown in Fig. 5. The result clearly shows a peak in all the plots, except in that the 3.2 g dl^{-1} solution. For this concentration, the q_m value in the early stage exists outside the measuring region, therefore the q_m cannot be directly confirmed. Besides, the experimental q_m values in Fig. 5 correspond well to the calculated values from the plot of $R(q)/q^2$ versus q^2. This fact directly indicates that the phase separation behavior of PVDF/TG solutions can be described using Cahn's theory. Fig. 6 shows the temperature dependence of the D_{app} value with various concentrations. From the intercept on the temperature axis, one can estimate the spinodal temperature, T_s, at which D_{app} is zero. Table 2 also shows this result.

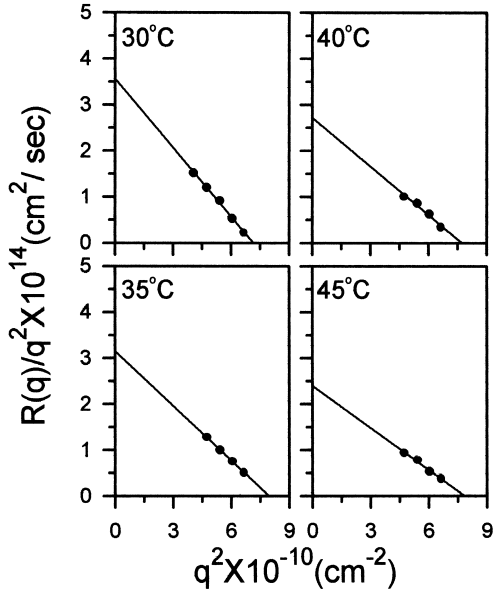

Fig. 4. Plot of $R(q)/q^2$ versus q^2 for 3.2 g dl^{-1} PVDF/TG solution at various temperatures.

Combining the results in the light scattering and the gelation kinetics, Fig. 7 shows the phase diagram of PVDF/TG solution. The sol–gel transition curve was determined by the critical gelation concentration and the gel-melting curve was estimated by the conventional test tube upside-down method. From the spinodal curve, it is confirmed that the phase separation in PVDF/TG solution is an upper critical solution temperature (UCST) type. The phase diagram of Fig. 7 is similar to that obtained from PVC/γ-butyrolactone solution as reported by Kawanishi et al. [17], which indicates the uniformity of the gelation behavior. One can divide the phase diagram into four regions using the sol–gel transition and spinodal decomposition curves. In the $T > T_s$ and $C < C^*_{gel}$ region, the solution is a homogeneous sol. When $T < T_s$ and $C < C^*_{gel}$, the solution should separate into two distinct phases but the gelation does not occur. The gel formation without liquid–liquid phase separation occurs in the $T > T_s$ and $C > C^*_{gel}$ region. Then, the gelation and phase separation should occur simultaneously in the $T < T_s$ and $C > C^*_{gel}$ region. The phase diagram as mentioned above, mainly revealed two kinds of gels according to the difference in the thermodynamic driving force. One is pure liquid–solid phase transition or crystallization in the $T > T_s$ and $C > C^*_{gel}$ region, the main junctions in the gel network are crystallites in nature [18]. On the other hand, the liquid–liquid phase separation proceeds and then the gelation/crystallization follows in $T < T_s$ and $C < C^*_{gel}$ region, since the liquid–liquid phase separation always takes place below the spinodal temperature in the UCST phase diagram. However, the gelation behavior in this region should become much complex because it is not possible to quantitatively investigate the gelation behavior simultaneously with phase separation by the equilibrium thermodynamic phase diagram. Therefore, we will further discuss the gelation kinetics in this region. The kinetic transition curve which is obtained by C^*_{trans} is supplemented into the phase diagram of Fig. 7. Now, below the sol–gel transition curve the phase diagram could be divided into three distinguishable gelation regions labeled as Gel(1), Gel(2) and Gel(3). For the Gel(1) region, the gelation occurs above the spinodal temperature. For the Gel(2) region, the gelation occurs simultaneously with liquid–liquid phase separation and the kinetic characteristic exponent value is approximately equal to 1. For the Gel(3) region, the gelation behavior and the thermodynamic condition is similar to Gel(2), but the kinetic characteristic exponent is equal to 2.

Table 2
Characteristic parameters describing spinodal decomposition of PVDF/TG solution

Conc. (g dl^{-1})	Temp. (°C)	D_{app} ($\times 10^{14}$ cm^2/s)	q_c ($\times 10^{-5}$ cm^{-1})	q_m ($\times 10^{-5}$ cm^{-1})	τ_0^{-1} ($\times 10^3$ s^{-1}[a])	T_s (°C)
3.2	30	3.56	2.67	1.89	2.53	76
	35	3.17	2.82	1.99	2.52	
	40	2.72	2.78	1.97	2.10	
	45	2.40	2.80	1.98	1.88	
4.2	30	3.54	2.84	2.01	2.85	
5.8	30	5.06	3.05	2.16	4.70	82
	40	4.54	3.02	2.14	4.14	
	50	3.20	3.01	2.13	2.9	
	60	2.16	2.86	2.02	1.77	
8.7	30	7.87	3.13	2.21	7.71	78
	40	7.36	3.12	2.20	7.16	
	50	5.97	3.10	2.19	5.74	
	60	3.39	2.96	2.09	2.97	
18.5	45	61.23	3.27	2.31	65.47	71
	50	50.25	3.19	2.26	51.13	
	55	35.43	3.16	2.23	35.38	
	64	18.51	3.12	2.21	17.67	

[a] The characteristic rate of the spinodal decomposition process, $\tau_0^{-1} = D_{app}q_c^2$.

4. Discussion

4.1. Gelation characterization in the Gel(1) region

It has often been reported [19,20] that the formation of a three-dimensional physical network in polymer solution through cross-linking process may be treated as a consecutive chemical reaction. Then, the intermolecular associations should overcome the activation energy barrier to form the junction points in the gel network. As stated earlier, the gel formation without liquid–liquid phase separation occurs in the Gel(1) region ($T > T_s$ and $C > C^*_{gel}$). Therefore, the gelation may occur directly through the liquid–solid phase transition by crystallite formation of the polymer chain segments. According to the pervious reports [18,21], the PVDF/TG gel gave the α-phase crystal structure containing two polymer chains with TGTḠ conformation in a unit cell. Hence we may presume the gelation mechanism in Gel(1) region. The kinetics of gelation process can be modeled as a consecutive chemical reaction. In this model the first step involves the two random coil chains in a solution which gather together to constitute an order domain, e.g. TGTḠ conformation, this step can be described as the elementary reaction. These order domains act as "nuclei" for the growth of fibrils, leading to the formation of junction points in the gel network. Hence, the gelation mechanism in Gel(1) region may be represented schematically as [19]:

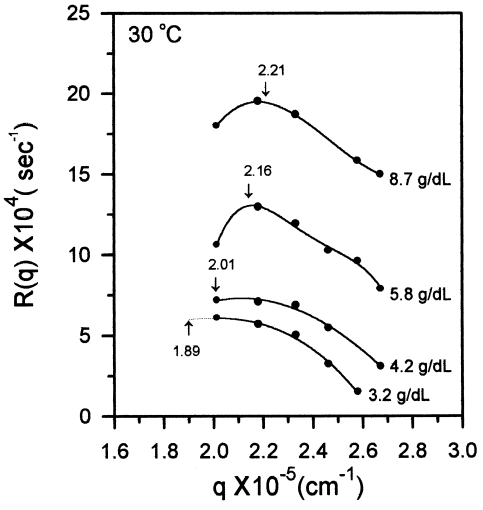

Fig. 5. Variation of growth rate $R(q)$ of spinodal decomposition with q measured for various concentrations at 40°C.

$$2(\text{polymer segments}) \xrightarrow{k_n} \text{nuclei} \rightarrow \text{cross-link} \quad (5)$$

where k_n is the nucleation rate constant. Assuming that the formation of nucleus is the rate-determining step in the gelation process, and the rate of overall reaction is governed just by the rate at which the nuclei are formed in this first step. According to the mass action law the rate equation of the overall reaction is

$$r_{Gel(1)} = k_n(C - C^*_{gel})^2 \quad (6)$$

where $r_{Gel(1)}$ is rate for the formation of cross-linking points per unit volume in the Gel(1) region and C^*_{gel} is the critical gelation concentration at a given gelation temperature. One can discuss the details of the rate constant, k_n, by the steady-state nucleation theory [22]. The rate constant of nucleation,

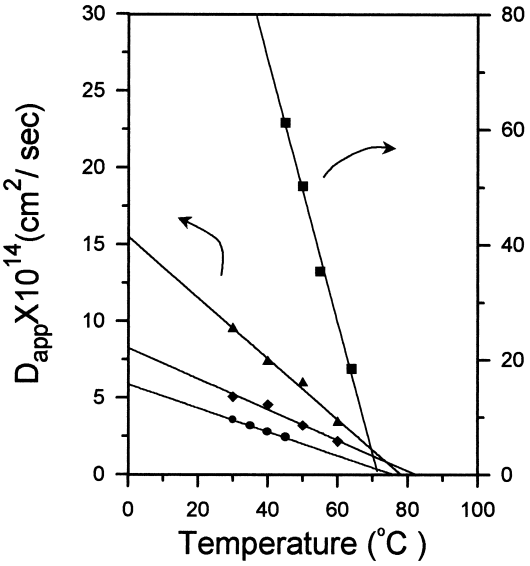

Fig. 6. Temperature dependence of the apparent diffusion coefficient, D_{app}, with various concentrations (in g dl^{-1}): (●) 3.2; (◆) 5.8; (▲) 8.7; (■) 18.5.

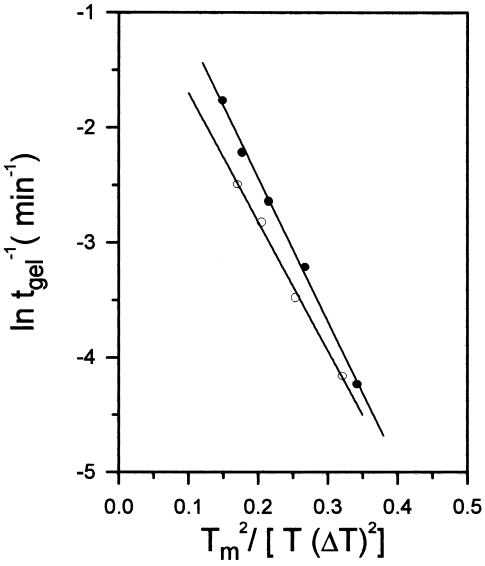

Fig. 8. Plot of $\ln t_{gel}^{-1}$ versus $T_m^2/[T(\Delta T)^2]$ for PVDF/TG solutions in the Gel(1) region: (●) 25 g dl^{-1}; (○) 20 g dl^{-1}.

k_n, is approximately given by

$$k_n = k' \exp\left[\left(\frac{-E_D}{RT}\right) + \left(\frac{-\Delta G^*}{k_B T}\right)\right] \tag{7}$$

where E_D is the free energy of activation for transport across the liquid–solid interface, ΔG^* is the Gibes free energy of formation of a critical nuclei from a solution, R is the gas constant, k_B is Boltzmann's constant, T is temperature and k' is a constant. If the thermodynamic potential barrier of nucleation determines the nucleation rate rather than the activation energy of the polymer segments that diffuse across the liquid–solid interface, i.e. $\Delta G^*/k_B T \gg E_D/RT$, we may write

$$k_n = k' \exp\left(\frac{-\Delta G^*}{k_B T}\right) \tag{8}$$

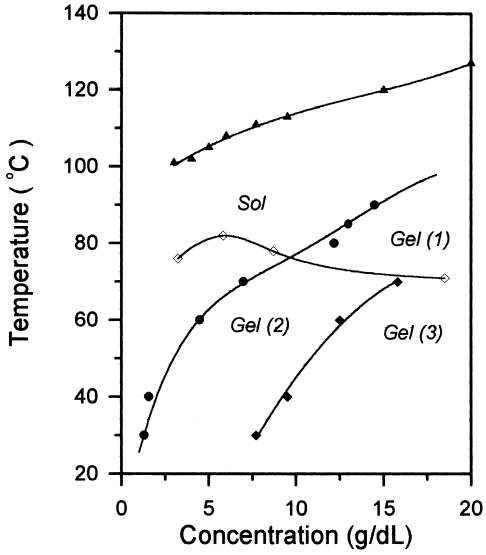

Fig. 7. Phase diagram of PVDF/TG solution: (●) sol–gel transition curve, which was obtained from C^*_{gel}; (◇) spinodal curve; (▲) gel melting curve; (■) kinetic transition curve, which was obtained from C^*_{trans}.

For the gelation from crystallization, the polymer chains have to form intermolecular association, which is structurally reminiscent of the fringed micelle model. The free energy of formation of the fringed micelle nucleus in polymer solutions has been suggested by Pinnings [23] and the thermodynamic barrier for the formation of critical nuclei, ΔG^*, can be obtained from following equation:

$$\Delta G^* = \frac{32\sigma_e\sigma_s^2 - (16/a)\sigma_s^2 k_B T \ln(v_p/x^{2\delta})T_m^2}{\Delta h_f^2 \Delta T^2} \tag{9}$$

We substitute Eq. (9) into Eq. (8) to obtain the rate constant of nucleation

$$k_n = k' \exp\left[\frac{-A(T)T_m^2}{k_B \Delta h_f^2 T \Delta T^2}\right] \tag{10}$$

where

$$A(T) = 32\sigma_e\sigma_s^2 - (16/a)\sigma_s^2 k_B T \ln(v_p/x^{2\delta})$$

where a is the cross-sectional surface area of a chain, and σ_e and σ_s are the surface free energies of the interfacial and the lateral per unit area, respectively. The logarithmic term represents the entropy of nucleation and arises from the spontaneous occurrence of a number of polymer chains localized by the nucleus. x is the number of segments of polymer chain and v_p is the volume fraction of the polymer. The parameter δ ($0 \le \delta \le 1/2$) was introduced to express the localization free energy of the chains protruding from

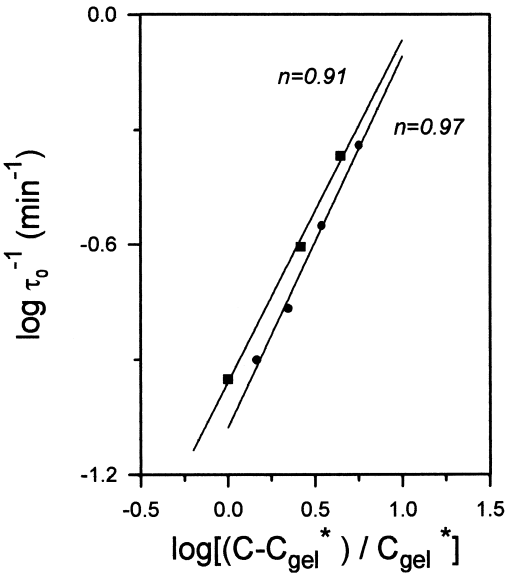

Fig. 9. Plot of log τ_0^{-1} versus log$[(C - C^*_{gel})/C^*_{gel}]$ for PVDF/TG solutions at the indicated temperatures: (●) 30°C; (■) 40°C.

the interface. Hence, t_{gel}^{-1} can be expressed by

$$t_{gel}^{-1} \propto r_{Gel(1)} \propto k' \exp\left[\frac{-A(T)T_m^2}{k_B \Delta h_f^2 T \Delta T^2}\right](C - C^*_{gel})^2 \qquad (11)$$

Fig. 8 shows a semi-logarithmic plot of ln t_{gel}^{-1} as a function of $T_m^2/[T(\Delta T^2)]$. Good linear relationships were obtained, indicating that the gelation in this region is confirmed by kinetic aspects, and that the mechanism of gelation is bimolecular association, controlled by the crystalline nucleation rate.

4.2. Gelation characterization in the Gel(2) region

In the Gel(2) region the liquid–liquid phase separation should always occur because of the thermodynamic driving force, $\partial^2 f/\partial C^2 < 0$. One can consider that the gel formation in this region was crystallization combined with liquid–liquid phase separation. This is considering that the phase separation takes place anteriorly and then followed by crystallization. Hence, the gelation mechanism in this region may be based on the analogy of heterogeneous reaction. For a general idea of the heterogeneous reaction, it would be expected for a mechanism in which the first step involves the process that polymer chains diffuse to create the polymer- and solvent-rich domains. The nucleation of polymer chains in the polymer-rich domain must be faster than that in the solvent-rich domain. Hence, the contribution of solvent-rich domain on the gelation process may be neglected. The rate equation can be deduced if we introduce the phase separation process into the consecutive reaction.

$$\text{homogeneous-solution} \xrightarrow{k_D} \text{heterogeneous-solution}$$

$$2(\textit{molecular chains in polymer-rich domain}) \xrightarrow{k_n} \text{nuclei} \qquad (12)$$

$$\rightarrow \text{cross-link}$$

where k_D is phase separation rate constant. As mentioned above, the kinetic characteristic exponent of the gelation process is about equal to 1 in the Gel(2) region. To see whether this characteristic exponent depends on the phase separation, we plot the characteristic rate of phase separation in the early stage, $\tau_0^{-1} = D_{app}q_c^2$, as a function of reduced concentration on a log–log scale in Fig. 9. An examination of Fig. 9 reveals a good straight line with a slope quite close to 1. This result clearly suggests that the gelation in the Gel(2) region is basically controlled by a phase separation process. Since the phase separation is the rate-determining step in the gelation process, the rate equation could be given as

$$r_{Gel(2)} = k_D(C - C^*_{gel}) \qquad (13)$$

This rate equation also indicates that the diffusion of polymer chains into polymer-rich domain from homogeneous solution can be similarly discussed by unimolecular heterogeneous reaction in solution. Considering that the driving force for the diffusion of polymer chains is due to spinodal decomposition. Hence

$$k_D \propto \tau_0^{-1} = D_{app}q_c^2 \qquad (14)$$

According to the linear theory of spinodal decomposition, the D_{app} and q_c^2 are given as

$$D_{app} = -D_c\left(\frac{\partial^2 f}{\partial C^2}\right); \qquad q_c^2 = -\frac{\partial^2 f/\partial C^2}{2\kappa} \qquad (15)$$

then k_D could be rewritten as

$$k_D \propto \frac{D_c}{2\kappa}\left(\frac{\partial^2 f}{\partial C^2}\right)^2 \qquad (16)$$

On the other hand, Van Aartsen [24] suggested that the $\partial^2 f/\partial C^2$ could be expressed by

$$\frac{\partial^2 f}{\partial C^2} = \frac{2RT}{\bar{v}_1}(\chi_{T_s} - \chi_T) \qquad (17)$$

where χ_T is the polymer–solvent interaction parameter at a given temperature T and $\bar{v}_1$ is the molar volume of the solvent. We substitute the interaction parameter, $\chi = A + (B\bar{v}_1/RT)$ where A and B are constants, into Eq. (17) to obtain

$$\frac{\partial^2 f}{\partial C^2} = 2B\left(\frac{T}{T_s} - 1\right) \qquad (18)$$

Substitution of Eq. (18) into Eq. (16) leads to

$$k_D \propto \frac{D_c}{2\kappa}\left[2B\left(\frac{T}{T_s} - 1\right)\right]^2 \qquad (19)$$

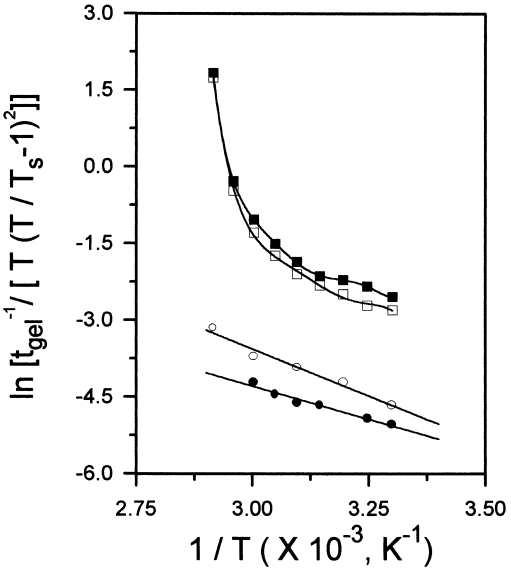

Fig. 10. Plot of $\ln\{t_{gel}^{-1}/[T(T/T_s-1)^2]\}$ versus $1/T$ for PVDF/TG gels at various concentrations (in g dl^{-1}): (●) 6; (○) 7; (□)15; (■) 17.

where D_c is the cooperative diffusion coefficient and T_s is the spinodal temperature. D_c can be evaluated using the Stokes–Einstein relation: $D_c = k_B T/6\pi\eta_0\xi$, where η_0 is the solvent viscosity and ξ is the correlation length. The temperature dependence of η_0 can be examined through the Arrhenius relation: $\eta_0 \propto \exp(E_a/RT)$, where E_a is the activation energy. Finally, the gelation rate, t_{gel}^{-1}, is proportional to $r_{Gel(2)}$ and is represented by the following equation

$$t_{gel}^{-1} \propto r_{Gel(2)} \propto \frac{B^2 k_B T}{3\pi\xi\kappa}\left(\frac{T}{T_s}-1\right)^2 \exp\left(\frac{-E_a}{RT}\right)(C - C^*_{gel}) \quad (20)$$

The influence of phase separation on gelation is borne out by Fig. 10, which shows a semi-logarithmic plot of $\ln\{t_{gel}^{-1}/[T(T/T_s-1)^2]\}$ as a function of $1/T$ from Eq. (20). It is clear that the observed values are very well fitted by straight lines for PVDF/TG solutions at the concentrations of 6 and 7 g dl^{-1}, indicating that the gelation behavior in the Gel(2) region is controlled mainly by thermodynamic driving force for the spinodal decomposition. On the other hand, a variance in the experimental result for concentrated PVDF solutions, 15 and 17 g dl^{-1}. This discrepancy may be attributed to the fact that the mechanism of gelation is not determined by the first step of phase-separation control in concentrated solutions.

4.3. Gelation characterization in the Gel(3) region

As discussed above, the slow phase-separation step followed by rapid nucleation process has been said to be diffusion controlled, because the rate of overall reaction is the same as the rate of the initial step of phase separation. On the other hand, the gelation behavior may be similarly described by the crystalline nucleation control, since the kinetic characteristic exponent is equal to 2 in the Gel(3) region. If the spinodal phase separation of concentrated solution is too fast compared with that of the nucleation in the second reaction, the concentration of polymer-rich phase must increase rapidly and then reach an equilibrium concentration. In other words, there must be a rapid pre-equilibrium of phase separation followed by a slow nucleation step. In order to obtain more detailed information on the gelation characteristics of the Gel(2) and Gel(3) regions, the relationship between the phase separation and the gelation time is shown in Fig. 11. In this result, the light-scattering measurement was carried out by rotating the test tube to reduce the effect of inhomogeneity of the sample. Fig. 11(a) shows the relationship between the phase separation and gelation behaviors for the Gel(2) region. The data for initial stage show that the exponential increase in the scattered intensity with time can be observed and described by Cahn's linear theory. With increasing time, the scattered intensity deviates from the exponential relationship. Comparing the results with the gelation kinetic, this deviation is considered due to the gel formation. In this region, the gelation takes place immediately after the initial phase separation. This result directly confirms that the phase separation process is the rate-determining step during gelation and agrees with the discussion in Section 4.2. As shown in Fig. 11(b), the gelation in Gel(3) occurs after the phase separation, i.e. the gel forms beyond the time evolution of spinodal decomposition from the exponential growth in early stage to intermediate or late stages. Hence, the scattered intensity

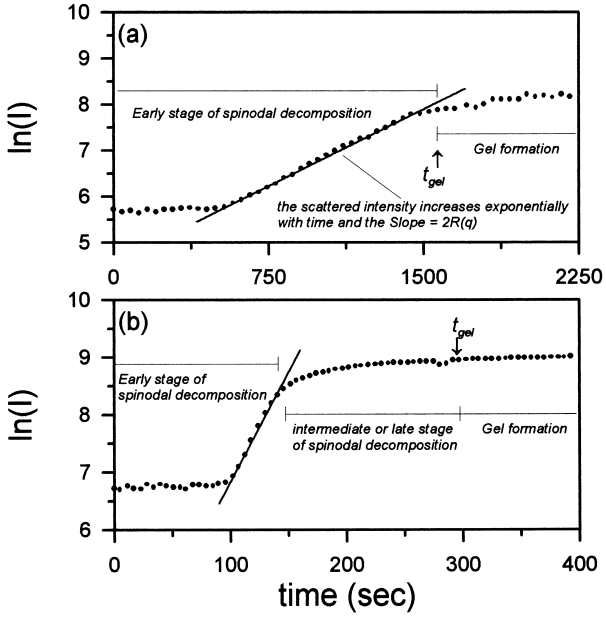

Fig. 11. Illustration of the relationship between phase separation and gelation behaviors: (a) 18.5 g dl^{-1} solution at 40°C (in Gel(3)); (b) 5.8 g dl^{-1} solution at 40°C (in Gel(2)).

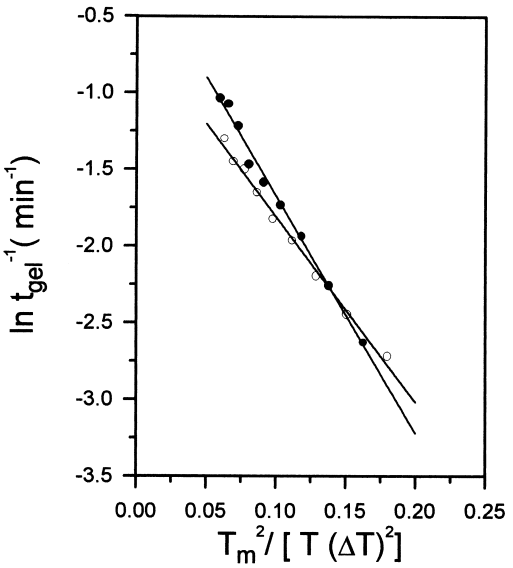

Fig. 12. Plot of $\ln t_{gel}^{-1}$ versus $T_m^2/[T(\Delta T)^2]$ for PVDF/TG solutions in the Gel(3) region at various concentrations (in g dl^{-1}): (○) 15; (●) 17.

deviation from the exponential relationship is considered a consequence of the coarsening effect at the late stage of spinodal decomposition. For this, we consider that there are two effects on gelation processes in the later stage of spinodal decomposition: (1) the concentration in the polymer-rich phase reaches the equilibrium concentration; and (2) with time evolution, the phase separation domain structure caused by the dynamic percolation-to-cluster transition has been suggested by Hasegawa et al. [26]. In the higher concentration region, i.e. in Gel(3), the effect of dynamic percolation-to-cluster transition can be neglected because the system always retains a continuous polymer-rich phase during the phase-separation process. Therefore, the kinetics of gelation only depends on the concentration of the polymer-rich domain. When this condition is satisfied, the assumption of pre-equilibrium during phase separation can be established.

If the nucleation process is the rate-determining step in the Gel(3) region, then the overall reaction rate can be written as

$$r_{\mathrm{Gel(3)}} = k_n(C_{\text{polymer-rich}} - C^*_{\mathrm{gel}})^2 \tag{21}$$

According to the equilibrium assumption [25] the nucleation rate is too slow to disturb the equilibrium homogeneous solution ↔ polymer-rich phase

$$(C_{\text{polymer-rich}} - C^*_{\mathrm{gel}}) = \frac{k_D}{k_{-D}}(C_{\text{homogeneous}} - C^*_{\mathrm{gel}}) \tag{22}$$

Insertion of Eq. (22) into Eq. (21) gives

$$r_{\mathrm{Gel(3)}} = \frac{k_n k_D^2}{k_{-D}^2}(C_{\text{homogeneous}} - C^*_{\mathrm{gel}})^2$$

$$= k_n K^2 (C_{\text{homogeneous}} - C^*_{\mathrm{gel}})^2 \tag{23}$$

where k_{-D} is the rate constant of the reverse reaction and $K = k_D/k_{-D}$ is the equilibrium constant for the pre-equilibrium. Finally, the gelation rate in the Gel(3) region can be represented by the following equation:

$$t_{\mathrm{gel}}^{-1} \propto r_{\mathrm{Gel(3)}} \propto K^2 k' \exp\left[\frac{-A(T)T_m^2}{k_B \Delta h_f^2 T \Delta T^2}\right] \times (C_{\text{homogeneous}} - C^*_{\mathrm{gel}})^2 \tag{24}$$

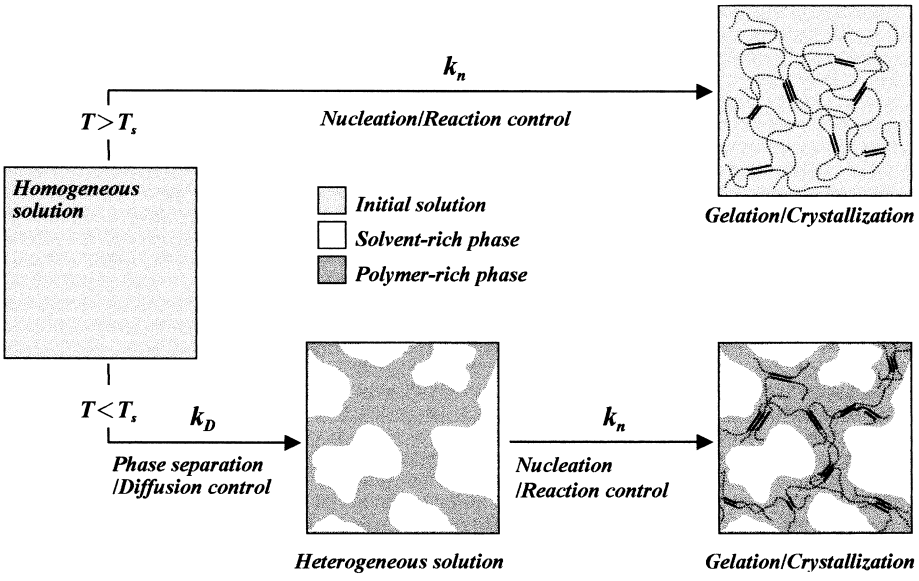

Fig. 13. Schematic picture of the initial gelation mechanism for PVDF/TG solution. According to the initial thermodynamic conditions, one can divide the gelation processes into two major parallel reactions. When $T > T_s$, the gelation should be virtually independent of phase separation and the gelation in terms of pure crystalline nucleation control. When $T < T_s$ and $k_D \ll k_n$, the phase separation process is the rate-determining step on gelation. When $T < T_s$ and $k_D \gg k_n$, then the crystalline nucleation process is the rate-determining step on gelation.

In the high-concentration region and in a narrow temperature range the contribution of K on the gelation rate is neglected and the K value can be considered as constant. Although this equation is a very rough approximation, it may be used to analyze the data in the Gel(3) region. Fig. 12 shows a semi-logarithmic plot of $\ln t_{gel}^{-1}$ versus $T_m^2/[T(\Delta T)^2]$ for PVDF/TG solutions at the concentration of 15 and 17 g dl^{-1}, respectively. The result shows clearly that the gelation in the Gel(3) region is in good agreement with the mechanism of crystalline nucleation control and bimolecular association in polymer solutions.

5. Conclusions

By using the various scattering techniques Takeshita et al. [27,28] have already proposed a good model for the hierarchic structure of PVA gel formed from the spinodal decomposition of the solution. However, the present study clarifies the effects of the crystallization and phase separation on the gelation of PVDF/TG solution in terms of thermodynamic and kinetic aspects. Combining the phase diagram with the kinetic analysis of the gelation processes, Fig. 13 shows the model of gelation mechanism in PVDF/TG solutions. According to the initial thermodynamic conditions, i.e. temperature, one can divide the gelation processes into two major parallel reactions. When the gelation temperature is above the spinodal temperature, the gelation should be virtually independent of phase separation and the gelation occurs in terms of pure crystalline nucleation control. When the gelation temperature is below the spinodal temperature, the liquid–liquid phase separation always occurs because of the thermodynamic driving force, $\partial^2 f/\partial C^2 < 0$. Therefore, the crystallization and phase separation should occur simultaneously and the gelation rate depends on the kinetic conditions in the competition between these two processes. When the gelation occurs at low concentration and high temperature ($k_D \ll k_n$), the phase separation process is the rate-determining step on gelation. The gelation in this region is said to be diffusion controlled. When the gelation occurs at high concentration and low temperature ($k_D \gg k_n$), the crystalline nucleation process is the rate-determining step on gelation. The gelation in this region is known as nucleation control or reaction control. This result also suggests that the influence of phase separation on gelation process may be weakened when the concentration is increased more than the kinetic transition concentration.

Acknowledgements

The authors would like to thank the National Science Council of the Republic of China for financially supporting this research under Contract No. NSC-89-2216-E-011-021.

References

[1] Hong PD, Chen JH. Polymer 1999;40:4077.
[2] Hong PD, Chen JH. Polymer 1998;39:711.
[3] Hong PD, Chou CM, Chen JH. Polymer 2000;41:5847.
[4] Banisil R, Lal J, Carvalho BL. Polymer 1992;33:2961.
[5] Matsuo M, Kawase M, Sugiura Y, Takematsu S, Hara C. Macromolecules 1993;26:4461.
[6] Tanigami T, Suzuki H, Yamaura K, Matsuzawa S. Macromolecules 1985;18:2595.
[7] Godard J, Biebuyck JJ, Dumerie M, Naveau H, Mercier JP. J Polym Sci Part B: Polym Phys 1978;16:1817.
[8] Coniglio A, Stanley HE, Klein W. Phys Rev Lett 1979;42:518.
[9] Tomura H, Saito H, Inoue T. Macromolecules 1992;25:1611.
[10] Ohkura M, Kanaya T, Kaji K. Polymer 1992;33:3686.
[11] Dikshit AK, Nandi AK. Macromolecules 1998;31:8886.
[12] Ohkura M, Kanaya T, Kaji K. Polymer 1992;33:5044.
[13] Cahn JW, Hilliadd JH. J Chem Phys 1958;28:258.
[14] Cahn JW. J Chem Phys 1965;42:93.
[15] Hashimoto T, Kumaki J, Kawai H. Macromolecules 1983;16:641.
[16] Lal J, Bansil R. Macromolecules 1991;24:290.
[17] Kawanishi K, Takeda Y, Inoue T. Polym J 1986;5:411.
[18] Voice AM, Davies GR, Ward IM. Polym Gels Networks 1997;5:123.
[19] Shibatain K. Polym J 1970;1:348.
[20] Mal S, Maiti P, Nandi AK. Macromolecules 1995;28:2371.
[21] Hasegawa R, Takahashi Y, Chatain Y, Tadokoro H. Polym J 1972;3:6000.
[22] Mandelkern L. Crystallization of polymers. New York: McGraw-Hill, 1964.
[23] Pennings AJ. J Polym Sci: Polym Symp 1977;59:55.
[24] Van Aartsen JJ. Eur Polym J 1970;6:919.
[25] Steinfeld JI, Francisco JS, Hase WL. Chemical kinetics and dynamics. Englewood Cliffs, NJ: Prentice-Hall, 1989.
[26] Hasegawa H, Shiwaku T, Nakai A, Hashimoto T. In: Komura S, Furukawa H, editors. Dynamics of ordering process in condensed matter, New York: Plenum Press, 1988.
[27] Takeshita H, Kanaya T, Kaji K, Nishida K, Nishikoji Y, Ohkura M. Kobunshi Ronbunshu 1998;55:595.
[28] Takeshita H, Kanaya T, Nishida K, Kaji K. Macromolecules 1999;32:7815.